

Article

Stability Analysis for Digital Redesign of Discrete-Time Switched Systems Using H_∞ Linear Matrix Inequality

Nien-Tsu Hu 

Graduate Institute of Automation Technology, National Taipei University of Technology, Taipei 10608, Taiwan; nthu@ntut.edu.tw

Abstract: In this paper, the stability problem for the digital redesign of discrete-time switched systems using H_∞ linear matrix inequality (LMI) is investigated. We propose the switching time approach for digital redesign between controller work and failure, and this switching time will limit the system output within the system capacity. When the controller fails, the overall system will be unstable. Therefore, if the digital redesign controller is not restored in a certain period of time, the system output will exceed the system capacity. To solve this problem, we propose a switching law to determine the switching time between the stable mode (controller work) and the unstable (controller failure) mode; this will limit the overall system states in the unstable mode. In addition, the digital redesign controller has the advantage of faster tracking. After we propose a discrete-time switching system with stable and unstable modes, we use H_∞ linear matrix inequality (LMI) and Lyapunov functions to prove the stability in detail. Finally, the numerical example illustrates the feasibility of the proposed approach.

Keywords: digital redesign; switched systems; linear matrix inequality; Lyapunov functions

MSC: 49N05; 93C57; 93D21



Citation: Hu, N.-T. Stability Analysis for Digital Redesign of Discrete-Time Switched Systems Using H_∞ Linear Matrix Inequality. *Mathematics* **2023**, *11*, 2468. <https://doi.org/10.3390/math11112468>

Academic Editor: Danilo Pelusi

Received: 1 May 2023

Revised: 22 May 2023

Accepted: 25 May 2023

Published: 27 May 2023



Copyright: © 2023 by the author. Licensee MDPI, Basel, Switzerland. This article is an open access article distributed under the terms and conditions of the Creative Commons Attribution (CC BY) license (<https://creativecommons.org/licenses/by/4.0/>).

1. Introduction

Many systems are dynamic systems that exhibit continuous and discrete dynamic behaviours. These systems that include two kinds of dynamic behaviour and interaction are called hybrid systems—for example, embedded systems, communication networks, and aircraft and traffic control. The history of hybrid systems began in the 1950s and attracted attention in the 1990s to implement the development of digital microcontrollers and embedded devices. Switched systems [1–8] are a special class of hybrid systems that might contain continuous-time or discrete-time subsystems and a switching law orchestrating switching between these subsystems and can be viewed as higher-level abstractions of hybrid systems.

In fact, many practical systems have multimodal dynamical subsystems to exhibit diversified behaviour, which might depend on various environments. In recent years, switched system research has seen an increasing trend and has made great efforts; see, e.g., [9–11]. The research is always focused on stability analysis and controller design to guarantee switched systems stability and achieve good performance. As we know, there are several methods applied to stability analysis of those systems, namely Lyapunov function [12–15], linear matrix inequality [16–18], and dwell time [19–21]. However, the above and recent studies have not discussed the stability analysis of the switching system based on the digital redesign in the stable mode and the unstable mode. This paper is based on the first and third cases and uses the H_∞ linear matrix inequality to cooperate with the piecewise Lyapunov method functions and the average dwell time to derive switching laws. In addition, the proposed switching law can be guaranteed to be convergent after the detailed proof in the Appendices A and B.

In terms of contributions, this paper successfully derives switching laws by H_∞ linear matrix inequality for unstable discrete-time switched systems and proves that state error can be bounded. Because state error is bounded, the system performance can also be bounded in a certain range. That tells us whether the controller will work or fail for an unstable discrete-time switched system, and we can know beforehand the approximate bound of system performance, which will be our expectation or not. Finally, the numerical example illustrates the feasibility of the proposed approach, and the robust performance and tracking performance for different Q values are shown in detail.

The stability problem for the digital redesign of discrete-time switched systems using H_∞ linear matrix inequality (LMI) is proposed in this paper. The proposed switching law is derived and strictly proves the stability. This paper is organized as follows. The switched system is briefly described along with H_∞ linear matrix inequality constraint in Section 2. The prediction-based digital redesign is introduced in Section 3. The main results and proofs are in Section 4, and an illustrative example is presented in Section 5 to demonstrate the effectiveness of the proposed methodology. Finally, the conclusion is addressed in Section 6.

2. Systems Description and Preliminaries

The stability analysis of the switched systems and the controller design have been our focus points in this paper, given the discrete-time switched systems [22] as follows:

$$\begin{cases} x(k+1) = A_{\sigma(k)}x(k) + B_{\sigma(k)}u(k), & x(0) = x_0 \\ y(k) = C_{\sigma(k)}x(k), \end{cases} \quad (1)$$

where $\sigma(k) : N^+ \rightarrow I_N = \{1, 2, \dots, N\}$, $N > 1$, N^+ denotes the set of all nonnegative integers, and $\sigma(k)$ is called a switching signal. N is the number of subsystems, which must be greater than 1, showing that it is N times that we switch over discrete-time switched systems (1). Every subsystem has its corresponding constant matrix, which gives A_i , B_i , and C_i ($i \in I_N$) to express. To simplify, all k represents kT , and $k_a - k_b$ represents $(k_a - k_b)T$ (T is the sampling time). Since all A_i or some A_i are stable, discrete-time switched systems, (1) can be exponentially stable under switching laws and satisfy the following inequality:

$$N_\sigma(0, k) \leq N_0 + \frac{k}{\tau}, \quad N_0 \geq 0, \quad \tau > 0, \quad (2)$$

where $N_\sigma(0, k)$ denotes the number of switching signals of $\sigma(k)$ on the interval $[0, k]$; τ is called the average dwell time; and N_0 is the chatter bound. For the concept of average dwell time, see [23]. For example, if $N_0 = 1$, then inequality (2) implies that $\sigma(k)$ cannot switch twice on any interval of length smaller than τ . Switching signals with this property are exactly the switching signals with dwell time τ . Note, also, that $N_0 = 0$ corresponds to the case of no switching since $\sigma(k)$ cannot switch at all on any interval of length smaller than τ . A detailed description is that consecutive switchings are separated by less than τ , but the average time interval between consecutive switchings is not less than τ . In general, if we discard the first N_0 switchings, then the average time interval between consecutive switchings is at least τ . We use the idea of average dwell time to derive a class of switching laws that exponentially stabilize the switched system (1) where both stable and unstable subsystems exist. As we obtain switching laws, we can know the upper and lower working time limits, which relate to controller design in the switched system (1).

For the controller design, we use the method of prediction-based digital redesign, and then our focal point is placed on utilizing H_∞ linear matrix inequality to cooperate with the piecewise Lyapunov method functions [24,25] and the preceding concept of average dwell time to derive switching laws. From [26–30], the H_∞ linear matrix inequality constraint is as follows:

Lemma 1 ([29]). Given any transfer function $G_i \equiv D_i + C_i(zI - A_i)^{-1}B_i$ (not necessarily minimal), we have

$$\|G_i\|_\infty < r_i,$$

A_i asymptotically stable.

If and only if the following LMI in P_i is feasible:

$$\begin{bmatrix} A_i^T P_i A_i - P_i & A_i^T P_i B_i & C_i^T \\ B_i^T P_i A_i & B_i^T P_i B_i - r_i I & D_i^T \\ C_i & D_i & -r_i I \end{bmatrix} < 0, P_i > 0 \tag{3}$$

Lemma 1 stipulates that all A_i must be asymptotically stable. In much research, A_i addresses the situation of asymptotically stable, but when discrete-time switched system (1) is not asymptotically stable, and the controller fails ($u(k) = 0$), how should we deal with this problem? To address this problem, this paper proposes a method to solve and prove that the norm of tracker error $e(k)$ is bounded in a certain range and derives switching laws suitable for unstable discrete-time switched systems (1).

3. The Prediction-Based Digital Redesign

3.1. Optimal Linearization

We apply the optimal linearization methodology [30] for generating optimal local models, which provides a tool for digital redesign for the class of time-varying nonlinear systems. This method is briefly described here and is used in the following.

Consider a class of nonlinear systems as follows:

$$\dot{x}(t) = f(x(t)) + g(x(t)) u(t), \tag{4}$$

where $f(\cdot) : \mathbb{R}^n \rightarrow \mathbb{R}^n$ and $g(\cdot) : \mathbb{R}^n \rightarrow \mathbb{R}^m$ are nonlinear functions; $x(t) \in \mathbb{R}^n$ is the state vector; and $u(t) \in \mathbb{R}^m$ is the control input. Assume that a local “linear model” (A_l, B_l) at the operation state, $x_l(t) \in \mathbb{R}^n$, is desired in the form

$$\dot{x}(t) = A_l x(t) + B_l u(t), \tag{5}$$

Assume that the operating state, $x_l \neq 0$, is not necessarily an equilibrium of the given system (4). One wishes to find two constant matrices A_l and B_l such that

$$f(x) + g(x) u \approx A_l x + B_l u \text{ for any } u, \tag{6}$$

$$f(x_l) + g(x_l) u_k = A_l x_l + B_l u \text{ for any } u. \tag{7}$$

$$g(x_l) = B_l. \tag{8}$$

Therefore, (6) and (7) can be reduced to a brief form as

$$f(x) \approx A_l x, \tag{9}$$

and

$$f(x_l) = A_l x_l. \tag{10}$$

To satisfy these, a_j^T is denoted as the j th row of the matrix A_l so that (9) and (10) can be represented as

$$f_j(x) \approx a_j^T x, j = 1, 2, \dots, n \tag{11}$$

and

$$f_j(x_l) = a_j^T x_l, j = 1, 2, \dots, n, \tag{12}$$

respectively, where $f_j(\cdot) : \mathbb{R}^n \rightarrow \mathbb{R}$ is the j th component of the vector $f(\cdot)$. Then, expanding the left-hand side of (11) about x_l and neglecting the second- and higher-order terms, we can obtain

$$f_j(x_l) + [\nabla f_j(x_l)]^T(x - x_l) \approx a_j^T x, \tag{13}$$

where $\nabla f_j(x_l) : \mathbb{R}^n \rightarrow \mathbb{R}^n$ is the gradient column vector of f_j evaluated at x_l . Now, using (12), one can rewrite (13) as

$$[\nabla f_j(x_l)]^T(x - x_l) \approx a_j^T(x - x_l)$$

in which x is arbitrary but should be close to x_l so that the approximation is good. To determine a constant vector, a_j^T , such that it is as close as possible to $[\nabla f_j(x_l)]^T$ and satisfies $a_j^T x_l = f_j(x_l)$, our objective can, thus, be formulated as a constrained optimization problem to minimize

$$E \equiv \frac{1}{2} \|\nabla f_j(x_l) - a_j\|_2^2 \text{ subject to } a_j^T x_l = f_j(x_l), \tag{14}$$

where a_j^T is the j th row of the matrix A_l . Note that this is also a convex-constrained optimization problem. Thus, using the Lagrange multiplier method, the optimal solution is

$$a_j = \nabla f_j(x_l) + \frac{f_j(x_l) + x_l^T \nabla f_j(x_l)}{\|x_l\|_2^2} \cdot x_l \text{ for } x_l \neq 0, \tag{15}$$

where $\|x_l\|_2^2 = x_l^T x_l$ is the square magnitude of the components of x_l .

The controllability matrix for the nonlinear system (4) at the operating state x_l is derived from the optimal linear model A_l, B_l , resulting in

$$\bar{C} = [\bar{B}_l \quad \bar{A}_l \bar{B}_l \quad \bar{A}_l^2 \bar{B}_l \quad \dots \quad \bar{A}_l^{n-1} \bar{B}_l], \tag{16}$$

where \bar{A}_l and \bar{B}_l are constructed via the following rule: the q th columns of A_l and B_l are set to zero whenever the q th component of x_l is zero.

Remark 1. ([31]). *It is well known that the high-gain property can suppress system uncertainties [31]. For this reason, the high-gain property is adopted in this paper.*

3.2. Linear-Quadratic Analogue Tracker Design

Consider a linear-quadratic analogue system described as

$$\begin{aligned} \dot{x}_c(t) &= A x_c(t) + B u_c(t) \\ y_c(t) &= C x_c(t) + D u_c(t), \quad x_c(0) = x_0 \end{aligned} \tag{17}$$

which is assumed to be both controllable and observable, where $x_c(t) \in \mathbb{R}^n, u_c(t) \in \mathbb{R}^m$, and $y_c(t) \in \mathbb{R}^p$. The optimal state-feedback control law minimizes the following performance index:

$$J = \int_0^\infty \left\{ [C x_c(t) - y_r(t)]^T Q [C x_c(t) - y_r(t)] + u_c^T(t) R u_c(t) \right\} dt, \tag{18}$$

with $Q \geq 0$ and $R > 0$ for system (17) with $D = 0$. This optimal control [31] is given by

$$u_c(t) = -K_c x_c(t) + E_c y_r(t). \tag{19}$$

The resulting closed-loop system becomes

$$\dot{x}_c(t) = (A - B K_c) x_c(t) + B E_c y_r(t), \tag{20}$$

where

$$K_c = R^{-1} B^T P, \tag{21}$$

$$E_c = -R^{-1} B^T [(A - B K_c)^{-1}]^T C^T Q. \tag{22}$$

Here, $y_r(t)$ is a reference input and P is the solution of the Riccati equation:

$$A^T P + P A - P B R^{-1} B^T P + C^T Q C = 0. \tag{23}$$

Remark 2. ([31]). It is noted that the high-gain property can be obtained by choosing a sufficiently high ratio of Q to R in (18) so that the system output can closely track the reference input. However, the high-gain property of the tracker usually yields large control signals, which might cause the system actuator to saturate and give an unsatisfactory system response. To achieve perfect performance, sometimes a search process is needed for the selection of the weighting matrices.

3.3. Observer-Based Linear-Quadratic Analogue Tracker Design

Consider the situation in which the system state of (17) cannot all be measured. Then, the observer can be used to estimate the unmeasured system state. Consider the linear observable continuous-time system in Figure 1, which is described as follows:

$$\dot{\hat{x}}_c(t) = A \hat{x}_c(t) + B u_c(t) + L [y_c(t) - C \hat{x}_c(t)] \tag{24}$$

where $\hat{x}_c(t)$ is the estimate of $x_c(t)$, and $L \in \mathbb{R}^{n \times p}$ is the observer gain. Let the estimation error be

$$\tilde{x}_c(t) = x_c(t) - \hat{x}_c(t), \tag{25}$$

which implies

$$\dot{\tilde{x}}_c(t) = \dot{x}_c(t) - \dot{\hat{x}}_c(t). \tag{26}$$

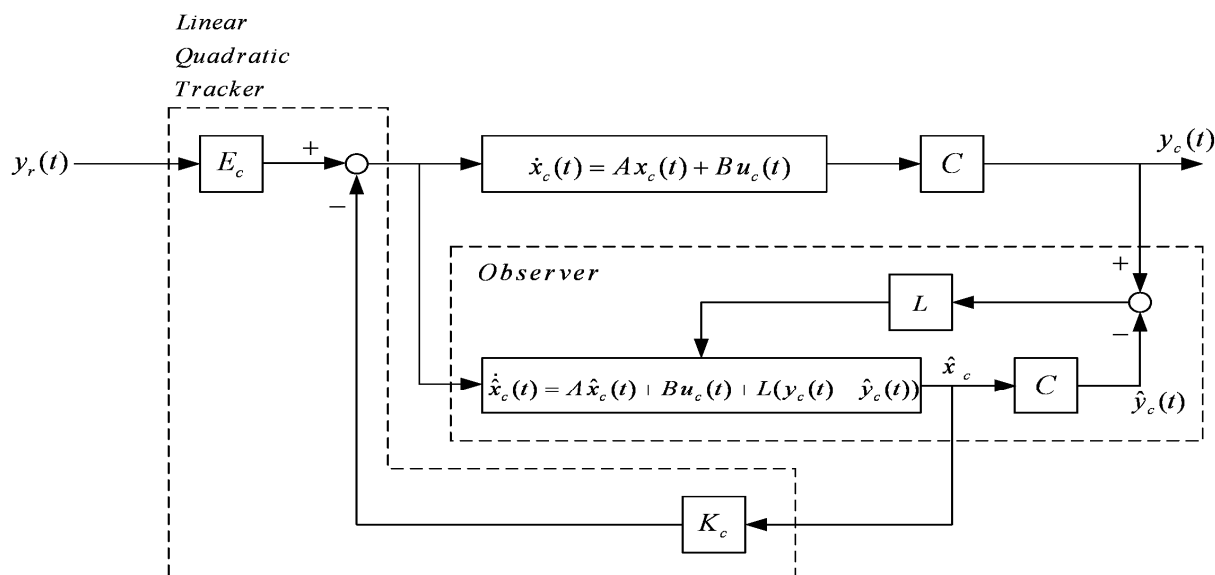


Figure 1. Observer-based linear-quadratic analogue tracker.

Substituting (17) with $D = 0$ and (24) into (26) yields

$$\dot{\tilde{x}}_c(t) = (A - L C) \tilde{x}_c(t), \tag{27}$$

which contrasts (20) and (27) with $y_r(t) = 0$. One can see that

$$(A - LC)^T = A^T - C^T L^T, \tag{28}$$

which has the structure as a state-feedback controller. The optimal control gain K_c can be used to select the observer gain L as follows:

$$L = K_c^T = P_{ob} C^T R_{ob}^{-1}, \tag{29}$$

where P_{ob} is the solution of the following Riccati equation:

$$A P_{ob} + P_{ob} A^T - P_{ob} C^T R_{ob}^{-1} C P_{ob} + Q_{ob} = 0, \tag{30}$$

in which $Q_{ob} \geq 0$, and $R_{ob} > 0$.

3.4. Digital Redesign of the Linear-Quadratic Analogue Tracker

Let the continuous-time state-feedback controller be

$$u_c(t) = -K_c x_c(t) + E_c y_r(t), \tag{31}$$

where $K_c \in \mathfrak{R}^{m \times n}$ and $E_c \in \mathfrak{R}^{n \times m}$ have been designed to satisfy some specified goals, and $y_r(t) \in \mathfrak{R}^m$ is a desired reference input vector. Thus, the analogously controlled system is

$$\dot{x}_c(t) = A_c x_c(t) + B E_c y_r(t), x_c(0) = x_{c0} = x_0, \tag{32}$$

where $A_c = A - B K_c$. Let the state equation of a corresponding discrete-time equivalent model be

$$\dot{x}_d(t) = A x_d(t) + B u_d(t), x_d(0) = x_{d0} = x_0, \tag{33}$$

where $u_d(t) \in \mathfrak{R}^m$ is a piecewise-constant input vector, satisfying

$$u_d(t) = u_d(kT), \text{ for } kT \leq t < (k + 1) T,$$

and $T > 0$ is the sampling period. Then, the discrete-time state-feedback controller is given by [30]

$$u_d(kT) = -K_d x_d(kT) + E_d y_r^*(kT) \tag{34}$$

where

$$K_d = (I_m + K_c H)^{-1} K_c G, \tag{35}$$

$$E_d = (I_m + K_c H)^{-1} E_c, \tag{36}$$

$$y_r^*(kT) = y_r(kT + T), \tag{37}$$

$$G = e^{A T}, \tag{38}$$

$$H = (G - I_n) A^{-1} B, \tag{39}$$

Whenever A^{-1} does not exist, H can be computed by the following formula [32]:

$$H = \sum_{v=1}^{\infty} \frac{1}{v!} (AT)^{v-1} B T.$$

The digitally controlled closed-loop system thus becomes

$$\begin{aligned} \dot{x}_d(t) &= A x_d(t) + B [-K_d x_d(kT) + E_d y_r^*(kT)], \quad x_d(0) = x_{d0}, \\ y_d(kT) &= C x_d(kT), \text{ for } kT \leq t < (k+1)T. \end{aligned} \tag{40}$$

Remark 3 (sampling period selection). It is noted that the mapping of a continuous-time system to its corresponding discretized system can be one-to-one if the selected sampling period satisfies the sampling theorem [33].

3.5. Digital Redesign of the Observer-Based Linear-Quadratic Analogue Tracker

Consider the linear observable continuous-time system

$$\dot{\hat{x}}_c(t) = A \hat{x}_c(t) + B u_c(t) + L [y_c(t) - C \hat{x}_c(t)], \tag{41}$$

by defining the continuous-time and discrete-time state estimate errors, respectively, as

$$\begin{aligned} \tilde{x}_c(t) &\equiv x_c(t) - \hat{x}_c(t), \\ \tilde{x}_d(kT) &\equiv x_d(kT) - \hat{x}_d(kT), \end{aligned} \tag{42}$$

then

$$\tilde{x}_d(kT) \approx \tilde{x}_c(t)|_{t=kT}.$$

Using the duality once again, the discrete-time state estimation error dynamics can be found as follows:

$$\tilde{x}_d(kT + T) = (G - MN) \tilde{x}_d(kT), \tag{43}$$

where

$$G = e^{AT}, \tag{44}$$

$$M = (G - I_n) A^{-1}L, \tag{45}$$

$$N = (I_m + CM)^{-1}CG. \tag{46}$$

Further define

$$L_d = M(I_m + CM)^{-1}, \tag{47}$$

then one has

$$MN = (G - I_n) A^{-1}L(I_m + CM)^{-1}CG = LCG. \tag{48}$$

Since

$$\begin{aligned} x_d(kT + T) &= G x_d(kT) + H u_d(kT), \\ y_d(kT) &= C x_d(kT), \end{aligned} \tag{49}$$

from (49), one has

$$CG x_d(kT) = y_d(kT + T) - CH u_d(kT). \tag{50}$$

Substituting (48) into (43) yields

$$\begin{aligned} \tilde{x}_d(kT + T) &= x_d(kT + T) - \hat{x}_d(kT + T) \\ &= (G - L_d CG)(x_d(kT) - \hat{x}_d(kT)) \\ &= (G - L_d CG) x_d(kT) - (G - L_d CG) \hat{x}_d(kT). \end{aligned} \tag{51}$$

Substituting (50) into (51), one has

$$\begin{aligned} \tilde{x}_d(kT + T) &= x_d(kT + T) - \hat{x}_d(kT + T) \\ &= [G x_d(kT) + H u_d(kT)] - \hat{x}_d(kT + T) \end{aligned} \tag{52}$$

$$\begin{aligned}
 &= G x_d(kT) - L_d [y_d(kT + T) - C H u_d(kT)] - (G - L_d C G) \hat{x}_d(kT) \\
 &= G x_d(kT) - L_d y_d(kT + T) + L_d C H u_d(kT) - (G - L_d C G) \hat{x}_d(kT).
 \end{aligned}
 \tag{53}$$

From (52) and (53), one has the discrete observer

$$\begin{aligned}
 \hat{x}_d(kT + T) &= (G - L_d C G) \hat{x}_d(kT) + (I_n - L_d C) H u_d(kT) + L_d y_d(kT + T) \\
 &= G_d \hat{x}_d(kT) + H_d u_d(kT) + L_d y_d(kT + T)
 \end{aligned}
 \tag{54}$$

and

$$\hat{y}_d(kT + T) = C \hat{x}_d(kT + T),$$

where

$$L_d = (G - I_n) A^{-1} L (I_m + C (G - I_n) A^{-1} L)^{-1},
 \tag{55}$$

$$G_d = G - L_d C G,
 \tag{56}$$

$$H_d = (I_n - L_d C) H,
 \tag{57}$$

$$G = e^{A T},
 \tag{58}$$

$$H = (G - I_n) A^{-1} B.
 \tag{59}$$

Considering the practical implementation, the following discrete observer using the current output $y_d(kT)$ and previously estimated state $\hat{x}_d(kT - T)$ to compute the currently estimated state $\hat{x}_d(kT)$ is suggested as an alternative:

$$\begin{aligned}
 \hat{x}_d(kT) &= G_d \hat{x}_d(kT - T) + H_d u_d(kT - T) + L_d y_d(kT), \\
 \hat{y}_d(kT) &= C \hat{x}_d(kT).
 \end{aligned}
 \tag{60}$$

The observer-based digital tracker and observer for the sampled-data optimal linear model are shown in Figure 2.

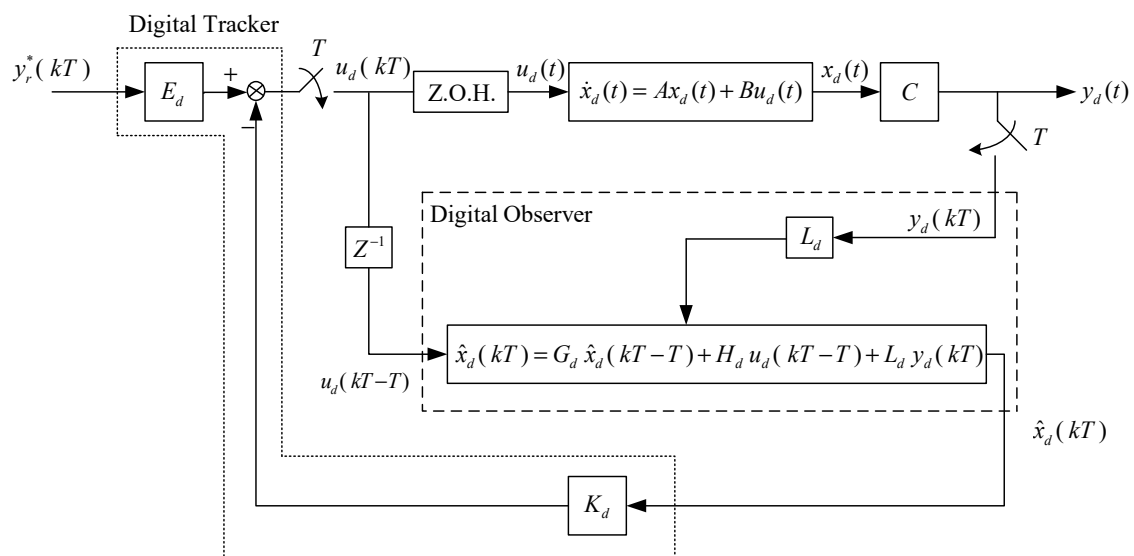


Figure 2. Prediction-based digital tracker and observer.

4. H_∞ Linear Matrix Inequality Constraint with An Unstable Discrete-Time System

We consider an unstable discrete-time system

$$\begin{cases} x_d(k+1) = A_d x_d(k) + B_d u_d(k), x_d(0) = x_0 \\ y_d(k) = C_d x_d(k), \end{cases} \tag{61}$$

where $A_d \in \mathbb{R}^{n \times n}$, $B_d \in \mathbb{R}^{n \times m}$, and $C_d \in \mathbb{R}^{p \times n}$ are system, input, and output matrices, respectively, and $x_d \in \mathbb{R}^n$, $u_d \in \mathbb{R}^m$, and $y_d \in \mathbb{R}^p$ are state, input, and output vectors. In the controller design, we utilize 3.2 small matters (21)~(23) with 3.4 small matters (34)~(39), where

$$G = e^{A T} = A_d, H = (G - I_n) A^{-1} B = B_d. \tag{62}$$

When the controller works, the unstable discrete-time system (61) changes into a stable discrete-time system as follows:

$$\begin{cases} x_d(k+1) = A_s x_d(k) + B_s y_r^*(k), x_d(0) = x_0 \\ y_d(k) = C_s x_d(k), \end{cases} \tag{63}$$

where $A_s = G - HK_d$, $B_s = HE_d$, and $C_s = C_d$. When the controller fails ($u_d(k) = 0$), the unstable discrete-time system (61) becomes

$$\begin{cases} x_d(k+1) = A_u x_d(k), x_d(0) = x_0 \\ y_d(k) = C_d x_d(k), \end{cases} \tag{64}$$

where $A_u = A_d$.

If the controller works, A_s is stable, and according to [27,28,34,35] and Lemma 1, the stable discrete-time system (63) will satisfy the following inequalities:

$$A_s^T P_s A_s - P_s < 0,$$

$$\begin{bmatrix} A_s^T P_s A_s - P_s & A_s^T P_s B_s & C_s^T \\ B_s^T P_s A_s & B_s^T P_s B_s - r_0 I & D_s^T \\ C_s & D_s & -r_0 I \end{bmatrix} < 0,$$

$$P_s > 0, \tag{65}$$

where $\|G_s\|_\infty < r_0$, $G_s \equiv D_s + C_s(zI - A_s)^{-1} B_s$. In inequality (65), the positive scalar λ_s ($\lambda_s < 1$) can exist and can be rewritten as follows:

$$A_s^T P_s A_s - \lambda_s^2 P_s < 0,$$

$$\begin{bmatrix} A_s^T P_s A_s - \lambda_s^2 P_s & A_s^T P_s B_s & C_s^T \\ B_s^T P_s A_s & B_s^T P_s B_s - r_0 I & D_s^T \\ C_s & D_s & -r_0 I \end{bmatrix} < 0,$$

$$P_s > 0. \tag{66}$$

Inequalities (66) can be equivalent to

$$A_s^T \Lambda_s A_s - \lambda_s^2 \Lambda_s < 0,$$

$$\begin{bmatrix} A_s^T \Lambda_s A_s - \lambda_s^2 \Lambda_s + C_s^T C_s & A_s^T \Lambda_s B_s + C_s^T D_s \\ B_s^T \Lambda_s A_s + D_s^T C_s & B_s^T \Lambda_s B_s - r_0^2 I + D_s^T D_s \end{bmatrix} < 0,$$

$$\Lambda_s > 0, \tag{67}$$

where $\Lambda_s = r_0 P_s$. The proof (66) to (67) is available in Appendix A.

Inequalities (67) can be used in the LMI control toolbox to obtain the solution of Λ_s . After the solution of Λ_s , we define the Lyapunov function candidate

$$\begin{aligned} V(x_d(k)) &= [C_s x_d(k) - y_r^*(k)]^T P_x [C_s x_d(k) - y_r^*(k)] \\ &= [x_d(k) - x_r^*(k)]^T \Lambda_s [x_d(k) - x_r^*(k)], \end{aligned} \tag{68}$$

where $P_x > \alpha I > 0$ ($\alpha > 0$), $y_r^*(k) = C_s x_r^*(k)$, and $\Lambda_s = C_s^T P_x C_s$. From (68), one obtains

$$\begin{aligned} &V(x_d(k+1)) - V(x_d(k)) \\ &= [x_d(k+1) - x_r^*(k)]^T \Lambda_s [x_d(k+1) - x_r^*(k)] - [x_d(k) - x_r^*(k)]^T \Lambda_s [x_d(k) - x_r^*(k)] \\ &= \{ [A_s x_d(k) + B_s y_r^*(k) - x_r^*(k)] \}^T \Lambda_s \{ [A_s x_d(k) + B_s y_r^*(k) - x_r^*(k)] \} - \\ &\quad [x_d(k) - x_r^*(k)]^T \Lambda_s [x_d(k) - x_r^*(k)] \\ &= \begin{bmatrix} x_d^T(k) & x_r^{*T}(k) \end{bmatrix} \begin{bmatrix} A_s^T \Lambda_s A_s - \Lambda_s & A_s^T \Lambda_s (B_s C_s - I) + \Lambda_s \\ (B_s C_s - I)^T \Lambda_s A_s + \Lambda_s & (B_s C_s - I)^T \Lambda_s (B_s C_s - I) - \Lambda_s \end{bmatrix} \begin{bmatrix} x_d(k) \\ x_r^*(k) \end{bmatrix}. \end{aligned} \tag{69}$$

By (67) and (69) can be represented as (see Appendix B)

$$V(x_d(k+1)) - V(x_d(k)) \leq (\lambda_s^2 - 1)V(x_d(k)) - c y_d^T(k) y_d(k) + (r_0^2 + \omega) y_r^{*T}(k) y_r^*(k), \tag{70}$$

where c ($c > 0$) is a scalar, and $\omega = \alpha(2\lambda_s^2 + 1)$. We can solve the inequality (70) to obtain

$$V(x_d(k)) \leq \lambda_s^{2(k-k_0)} V(x_d(k_0)) - \sum_{j=k_0}^{k-1} \lambda_s^{2(k-1-j)} \Gamma(j), \tag{71}$$

where $\Gamma(j) = c y_d^T(j) y_d(j) - (r_0^2 + \omega) y_r^{*T}(j) y_r^*(j)$, and inequality (71) denotes the Lyapunov function with the controller working over the interval $[k_{2i}, k_{2i+1})$.

Assume the controller of the unstable discrete-time system (61) works over the interval $[k_{2i}, k_{2i+1})$ and fails over the interval $[k_{2i+1}, k_{2i+2})$, where $i = 0, 1, 2, 3 \dots$, and $k_0 = 0$. Now, we first consider that working time k is located in the interval $[k_0, k_1)$ and use the following theorem (see [6]):

$$\alpha_1 \|x_d(k) - x_r^*(k)\|^2 \leq V(x_d(k)) \leq \alpha_2 \|x_d(k) - x_r^*(k)\|^2, \forall x_d, x_r^* \in \mathfrak{R}^n \tag{72}$$

where $\alpha_1 = \lambda_m(\Lambda_s)$, $\alpha_2 = \lambda_M(\Lambda_s)$, $\lambda_m(\cdot)$, $\lambda_M(\cdot)$ denotes the smallest (largest) eigenvalue of a symmetric matrix, and then

$$V(x_d(k)) \geq \alpha_1 \|x_d(k) - x_r^*(k)\|^2, V(x_d(k_0)) \leq \alpha_2 \|x_d(k_0) - x_r^*(k_0)\|^2. \tag{73}$$

From (71) and (73), we can obtain

$$\begin{aligned} \alpha_1 \|x_d(k) - x_r^*(k)\|^2 &\leq V(x_d(k)) \\ &= \lambda_s^{2(k-k_0)} V(x_d(k_0)) - \sum_{j=k_0}^{k-1} \lambda_s^{2(k-1-j)} \Gamma(j) \\ &\leq \lambda_s^{2(k-k_0)} \alpha_2 \|x_d(k_0) - x_r^*(k_0)\|^2 - \sum_{j=k_0}^{k-1} \lambda_s^{2(k-1-j)} \Gamma(j), \end{aligned} \tag{74}$$

and then

$$\|x_d(k) - x_r^*(k)\| \leq \sqrt{\mu \lambda_s^{2(k-k_0)} \|x_d(k_0) - x_r^*(k_0)\|^2 - \sum_{j=k_0}^{k-1} \lambda_c \lambda_s^{2(k-1-j)} \Gamma(j)}, \tag{75}$$

where $\mu = \frac{\alpha_2}{\alpha_1}$ and $\lambda_c = \frac{1}{\alpha_1}$. If $k \rightarrow k_1$, we can obtain

$$\|x_d(k_1) - x_r^*(k_1)\| \leq \sqrt{\mu \lambda_s^{2(k_1-k_0)} \|x_d(k_0) - x_r^*(k_0)\|^2 - \sum_{j=k_0}^{k_1-1} \lambda_c \lambda_s^{2(k_1-1-j)} \Gamma(j)}. \tag{76}$$

When the interval is $[k_0, k_1)$ to $[k_1, k_2)$, the controller works to fail, and a stable discrete-time system (63) will switch to an unstable discrete-time system (64). Thus, we can know

$$x_d(k) = A_u^{k-k_1} x_d(k_1). \tag{77}$$

System (76) is unstable, which causes system performances and states to grow quickly. To solve this problem, we assume there always exists λ_u ($\lambda_u \geq 1$), such that

$$\|A_u^q\| \leq h_u \lambda_u^q, \tag{78}$$

holds for $\forall q \geq 1$, where h_u is a constant scalar. From (78), we obtain

$$\|A_u^{k-k_1}\| \leq \lambda_u^{k-k_1}, \tag{79}$$

here we set $h_u = 1$. From (77) and (79), one obtains

$$\|x_d(k)\| \leq \lambda_u^{k-k_1} \|x_d(k_1)\|. \tag{80}$$

Because

$$\|x_d(k_1)\| - \|x_r^*(k_1)\| \leq \|x_d(k_1) - x_r^*(k_1)\| \leq \sqrt{\mu \lambda_s^{2(k_1-k_0)} \|x_d(k_0) - x_r^*(k_0)\|^2 - \sum_{j=k_0}^{k_1-1} \lambda_c \lambda_s^{2(k_1-1-j)} \Gamma(j)}, \tag{81}$$

we obtain

$$\|x_d(k_1)\| \leq \sqrt{\mu \lambda_s^{2(k_1-k_0)} \|x_d(k_0) - x_r^*(k_0)\|^2 - \sum_{j=k_0}^{k_1-1} \lambda_c \lambda_s^{2(k_1-1-j)} \Gamma(j)} + \|x_r^*(k_1)\|. \tag{82}$$

Combining (80) and (82), we can obtain the following inequality:

$$\begin{aligned} \|x_d(k)\| &\leq \lambda_u^{k-k_1} \|x_d(k_1)\| \\ &= \sqrt{\mu \lambda_u^{2(k-k_1)} \lambda_s^{2(k_1-k_0)} \|x_d(k_0) - x_r^*(k_0)\|^2 - \sum_{j=k_0}^{k_1-1} \lambda_c \lambda_u^{2(k-k_1)} \lambda_s^{2(k_1-1-j)} \Gamma(j)} + \lambda_u^{k-k_1} \|x_r^*(k_1)\| \\ &\leq \sqrt{\mu \lambda_u^{2(k-k_1)} \lambda_s^{2(k_1-k_0)} \|x_d(k_0) - x_r^*(k_0)\|^2 - \sum_{j=k_0}^{k_1-1} \lambda_c \lambda_u^{2(k-k_1)} \lambda_s^{2(k_1-1-j)} \Gamma(j)} + \|x_r^*(k)\|, \end{aligned} \tag{83}$$

and then

$$\|x_d(k) - x_r^*(k)\| \leq \sqrt{\mu \lambda_u^{2(k-k_1)} \lambda_s^{2(k_1-k_0)} \|x_d(k_0) - x_r^*(k_0)\|^2 - \sum_{j=k_0}^{k_1-1} \lambda_c \lambda_u^{2(k-k_1)} \lambda_s^{2(k_1-1-j)} \Gamma(j)}. \tag{84}$$

If $k \rightarrow k_2$, we can obtain

$$\|x_d(k_2) - x_r^*(k_2)\| \leq \sqrt{\mu \lambda_u^{2(k_2-k_1)} \lambda_s^{2(k_1-k_0)} \|x_d(k_0) - x_r^*(k_0)\|^2 - \sum_{j=k_0}^{k_1-1} \lambda_c \lambda_u^{2(k_2-k_1)} \lambda_s^{2(k_1-1-j)} \Gamma(j)}. \tag{85}$$

Similarly, when the working time k is located in the interval $[k_2, k_3)$, we repeat steps similar to (73)~(75) and utilize (85) to obtain

$$\|x_d(k) - x_r^*(k)\| \leq \frac{\|x_d(k_0) - x_r^*(k_0)\|}{\sqrt{\mu^2 \lambda_u^{2(k_2-k_1)} \lambda_s^{2(k-k_2+k_1-k_0)} - \sum_{j=k_0}^{k_1-1} \mu \lambda_c \lambda_u^{2(k_2-k_1)} \lambda_s^{2(k-k_2+k_1-1-j)} \Gamma(j) - \sum_{j=k_2}^{k-1} \lambda_c \lambda_s^{2(k-1-j)} \Gamma(j)}} \quad (86)$$

If $k \rightarrow k_3$, we can obtain

$$\|x_d(k_3) - x_r^*(k_3)\| \leq \frac{\|x_d(k_0) - x_r^*(k_0)\|}{\sqrt{\mu^2 \lambda_u^{2(k_2-k_1)} \lambda_s^{2(k_3-k_2+k_1-k_0)} - \sum_{j=k_0}^{k_1-1} \mu \lambda_c \lambda_u^{2(k_2-k_1)} \lambda_s^{2(k_3-k_2+k_1-1-j)} \Gamma(j) - \sum_{j=k_2}^{k_3-1} \lambda_c \lambda_s^{2(k_3-1-j)} \Gamma(j)}} \quad (87)$$

When the working time k is located in the interval $[k_3, k_4)$, we repeat (77)~(84) and utilize (87). We can obtain

$$\|x_d(k) - x_r^*(k)\| \leq \frac{\|x_d(k_0) - x_r^*(k_0)\|}{\sqrt{\mu^2 \lambda_u^{2(k-k_3+k_2-k_1)} \lambda_s^{2(k_3-k_2+k_1-k_0)} - \sum_{j=k_0}^{k_1-1} \mu \lambda_c \lambda_u^{2(k-k_3+k_2-k_1)} \lambda_s^{2(k_3-k_2+k_1-1-j)} \Gamma(j) - \sum_{j=k_2}^{k_3-1} \lambda_c \lambda_u^{2(k-k_3)} \lambda_s^{2(k_3-1-j)} \Gamma(j)}} \quad (88)$$

By repeatedly working, we can find that the error $\|x_d(k) - x_r^*(k)\|$ of the unstable discrete-time switched system (61) is limited whether the controller works or not, and the general form is

$$\|x_d(k) - x_r^*(k)\| \leq \sqrt{\mu^{I_d(0,k)} \lambda_u^{2K_u(0,k)} \lambda_s^{2K_s(0,k)} \|x_d(k_0) - x_r^*(k_0)\|^2 - \sum_{q=0,2,4,\dots} \left(\sum_{j=k_q}^{k-1(k_{q+1}-1)} \mu^{I_d(j,k)-1} \lambda_c \lambda_u^{2K_u(k_q,k)} \lambda_s^{2K_s(j,k)} \Gamma(j) \right)}, \quad (89)$$

$k \geq 0$.

We set $e(k) = x_d(k) - x_r^*(k)$, then (89) can be written as

$$\|e(k)\| \leq \sqrt{\mu^{I_d(0,k)} \lambda_u^{2K_u(0,k)} \lambda_s^{2K_s(0,k)} \|e(k_0)\|^2 - \sum_{q=0,2,4,\dots} \left(\sum_{j=k_q}^{k-1(k_{q+1}-1)} \mu^{I_d(j,k)-1} \lambda_c \lambda_u^{2K_u(k_q,k)} \lambda_s^{2K_s(j,k)} \Gamma(j) \right)}, \quad k \geq 0 \quad (90)$$

where $\Gamma(j) = cy_d^T(j)y_d(j) - (r_0^2 + \omega)y_r^{*T}(j)y_r^*(j)$. $K_u(a, b)$ and $K_s(a, b)$ denote all the controller working and failure times, respectively, in the interval $[a, b)$.

We define $N_\sigma(a, b)$ as the switched number in the interval $[a, b)$ and $I_d(a, b)$ as the corresponding constant. The relation that $N_\sigma(a, b)$ corresponds to $I_d(a, b)$ is as follows:

$$N_\sigma(a, b) : \begin{matrix} \boxed{01} & \boxed{23} & \boxed{45} & \dots \\ \downarrow & \downarrow & \downarrow & \dots \\ I_\sigma(a, b) : & 1 & 2 & 3 & \dots \end{matrix}$$

The general solution (90) of all states reflects all conditions where the controller works or fails. In the next study, we prove that all states of the switched system (61) can be bounded by L_2 and that the response is limited in a certain range.

Considering (90), set $e(k_0) = 0$.

Case 1: When $\mu = 1$, because $\|e(k)\| \geq 0$, from (90), we know that

$$\sum_{q=0,2,4,\dots} \left(\sum_{j=k_q}^{k-1(k_{q+1}-1)} \lambda_u^{2K_u(k_q,k)} \lambda_s^{2K_s(j,k)} \Gamma(j) \right) \leq 0. \quad (91)$$

If there exists a positive number λ^* , then

$$\lambda_u^{2K_u(k_q,k)} \lambda_s^{2K_s(j,k)} \leq \lambda^{*2(K_u(k_q,k)+K_s(j,k))} \quad (92)$$

holds. We set $j = 0, k_q = 0$ and then

$$\ln\left(\lambda_u^{2K_u(0,k)} \lambda_s^{2K_s(0,k)}\right) \leq \ln\left(\lambda^{*2(K_u(0,k)+K_s(0,k))}\right), \tag{93}$$

because $k = K_s(0,k) + K_u(0,k)$, we obtain the switching law from (93)

$$\frac{K_u(0,k)}{k} \leq \frac{\ln \lambda^* - \ln \lambda_s}{\ln \lambda_u - \ln \lambda_s}. \tag{94}$$

We observe (91); when $q = 0$ (or $q = 2, 4 \dots$), we sum (91) from $k = 1$ to $k = \infty$, then

$$\sum_{k=1}^{\infty} \left(\sum_{j=0}^{k-1} \lambda_u^{2K_u(0,k)} \lambda_s^{2K_s(j,k)} \Gamma(j) \right) = \sum_{j=0}^{\infty} \Gamma(j) \left(\sum_{k=j+1}^{\infty} \lambda_u^{2K_u(0,k)} \lambda_s^{2K_s(j,k)} \right) \leq 0. \tag{95}$$

Because

$$\sum_{k=j+1}^{\infty} \lambda_u^{2K_u(0,k)} \lambda_s^{2K_s(j,k)} > 0, \tag{96}$$

then

$$\sum_{j=0}^{\infty} \Gamma(j) \leq 0. \tag{97}$$

Inequality (97) denotes

$$\sum_{j=0}^{\infty} y_d^T(k) y_d(k) \leq \left(\frac{r_0^2 + \omega}{c} \right) \sum_{j=0}^{\infty} y_r^{*T}(k) y_r^*(k). \tag{98}$$

This result tells us that an L_2 gain $\frac{r_0^2 + \omega}{c}$ is achieved for the switching system under the switching law. Thus, the switching system is bounded by L_2 .

Case 2: When $\mu > 1$ and $j = 0, k_q = 0$, we obtain

$$\begin{aligned} \mu^{I_d(0,k)-1} \lambda_u^{2K_u(0,k)} \lambda_s^{2K_s(0,k)} &\leq \mu^{I_d(0,k)-1} \lambda^{*2(K_u(0,k)+K_s(0,k))} \\ &= \mu^{I_d(0,k)-1} \lambda^{*2k}. \end{aligned} \tag{99}$$

If there exists a positive number λ , then

$$\mu^{I_d(0,k)-1} \lambda^{*2k} \leq \lambda^{2k}. \tag{100}$$

We can obtain another switching law as follows:

$$I_d(0,k) \leq \frac{2k(\ln \lambda - \ln \lambda^*)}{\ln \mu} + 1, \quad \tau = \frac{\ln \mu}{2(\ln \lambda - \ln \lambda^*)}, \quad N_0 = 1. \tag{101}$$

We know that the average time between consecutive switching is larger than or equal to τ and (90) still holds from (101). Imitating the Case 1 proof, we know that Case 2 is also bounded by L_2 .

The above discussion is $e(k_0) = 0$. If the initial state $e(k_0) \neq 0$, because we care about the same terms (91) and (99), we can obtain the same switching laws (94) and (101). The different part is that the term $\mu^{I_d(0,k)} \lambda_u^{2K_u(0,k)} \lambda_s^{2K_s(0,k)} \|e(k_0)\|^2$ in (90) can be ignored. Combining the above analysis and results, we successfully provide switching laws and know that we can effectively bound the states of the unstable discrete-time system (61) under the switching laws. Inequalities (94) and (101) are our important results, and we combine them with the digital redesign method to simulate an example.

5. An Illustrative Example

In this section, we study an example to apply to this paper’s result. Consider an unstable MIMO continuous-time system as follows:

$$\begin{cases} \dot{x}_c(t) = \begin{bmatrix} -9.996 & -3.41 & 2.641 \\ 0 & -7.985 & 5.157 \\ 0 & 0 & 1.043 \end{bmatrix} x_c(t) + \begin{bmatrix} 0.987 & 0.016 \\ -0.011 & 0.99 \\ 1.043 & 1.043 \end{bmatrix} u_c(t), x_c(0) = [0 \ 0 \ 0], \\ y_c(t) = \begin{bmatrix} 1 & 0 & 0 \\ 0 & 1 & 0 \end{bmatrix} x_c(t). \end{cases} \tag{102}$$

The optimal controller (19) is given by

$$u_c(t) = -K_c x_c(t) + E_c y_r(t),$$

for $Q = 10^5 I_2$ and $R = I_2$ where

$$K_c = \begin{bmatrix} 306.266 & -4.528 & 2.584 \\ 1.293 & 308.346 & 5.105 \end{bmatrix}, \text{ and } E_c = \begin{bmatrix} 316.069 & -1.212 \\ 1.215 & 316.223 \end{bmatrix}.$$

The corresponding discrete-time model is

$$\begin{cases} x_d(kT + T) = \begin{bmatrix} 0.368 & -0.139 & 0.126 \\ 0 & 0.45 & 0.377 \\ 0 & 0 & 1.11 \end{bmatrix} x_d(kT) + \begin{bmatrix} 0.071 & 0 \\ 0.021 & 0.09 \\ 0.11 & 0.11 \end{bmatrix} u_d(kT), x_d(0) = [0 \ 0 \ 0], \\ y_d(kT) = \begin{bmatrix} 1 & 0 & 0 \\ 0 & 1 & 0 \end{bmatrix} x_d(kT), \end{cases} \tag{103}$$

where $T = 0.1$ s. The digital redesign controller is

$$u_d(kT) = -K_d x_d(kT) + E_d y_r^*(kT),$$

where

$$K_d = \begin{bmatrix} 4.908 & -1.917 & 1.753 \\ -1.177 & 5.193 & 3.738 \end{bmatrix}, \text{ and } E_d = \begin{bmatrix} 13.763 & 0.005 \\ -3.305 & 10.786 \end{bmatrix}.$$

Depending on whether the controller works well or fails, the corresponding switched forms of the system (103) will be similar to (63) or (64), where

$$\begin{aligned} A_s = G - HK_d &= \begin{bmatrix} 0.0195 & -0.002 & 0.001 \\ 0.002 & 0.022 & 0.003 \\ -0.41 & -0.36 & 0.505 \end{bmatrix}, B_s = HE_d = \begin{bmatrix} 0.977 & 0.0004 \\ -0.008 & 0.97 \\ 1.15 & 1.187 \end{bmatrix} \\ A_u = A_d = G &= \begin{bmatrix} 0.368 & -0.139 & 0.126 \\ 0 & 0.45 & 0.377 \\ 0 & 0 & 1.11 \end{bmatrix}, C_s = C_d = C = \begin{bmatrix} 1 & 0 & 0 \\ 0 & 1 & 0 \end{bmatrix}. \end{aligned}$$

To satisfy the H_∞ linear matrix inequalities in (66), set $r_0 = 2$ and choose parameters $\lambda_s = 0.9$, $\lambda_u = 3.8$, $\lambda^* = 1.65$, and $\lambda = 1.7$. By using the LMI control toolbox, we can obtain P_s and

$$\Lambda_s = \begin{bmatrix} 4.2 & 0.096 & -0.517 \\ 0.096 & 4.92 & -0.632 \\ -0.517 & -0.632 & 0.898 \end{bmatrix}$$

and then $\mu = \frac{\lambda_M(\Lambda_s)}{\lambda_m(\Lambda_s)} \cong 6.9$. According to (94) and (101), one has the switching laws for the controller working and not, respectively, as

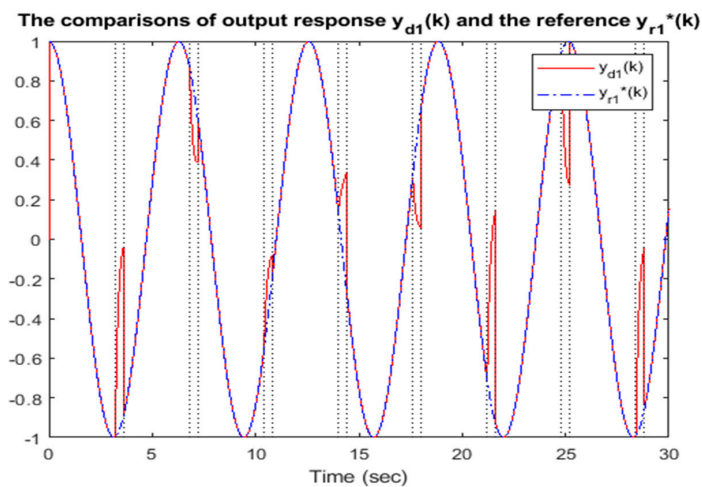
Switching law 1:

$$\tau = \frac{\ln \mu}{2(\ln \lambda - \ln \lambda^*)} = 31.428, \tau T \cong 3.1$$

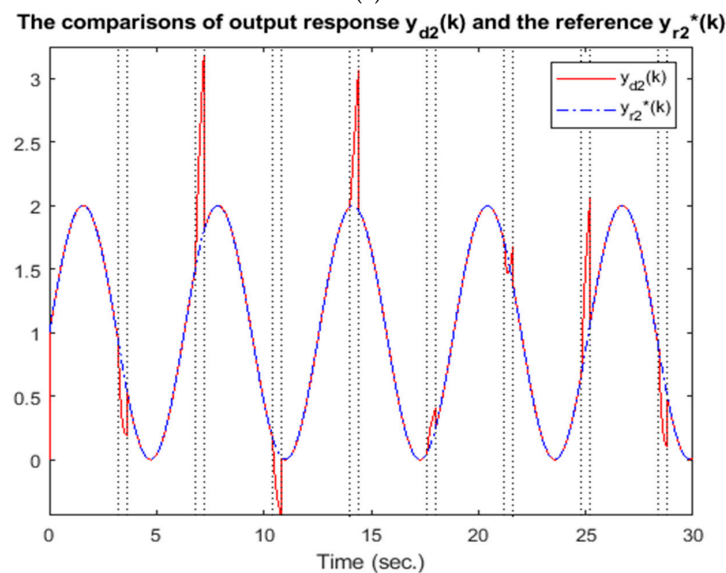
Switching law 2:

$$\frac{K_u(0, k)}{k} \leq \frac{\ln \lambda^* - \ln \lambda_s}{\ln \lambda_u - \ln \lambda_s} \cong 0.4.$$

Switching law 1 denotes the minimum value of the average time interval, which must be greater than or equal to 3.1, and switching law 2 denotes the unavailability rate of the switched system (103) with controller failure. We use switching laws to simulate the tracking of a switched system (103). Here, we choose 0.4 s for which the switched system (103) controller works and 3.2 s for which the controller fails. Figure 3a,b show the comparisons of the output response and the reference, where the reference $y_r^* = \begin{bmatrix} \cos(t) \\ 1 + \sin(t) \end{bmatrix}$, the sampling time $T = 0.1$ s, the initial state $x_d(0) = 0$, and the simulation time is 30 s.



(a)



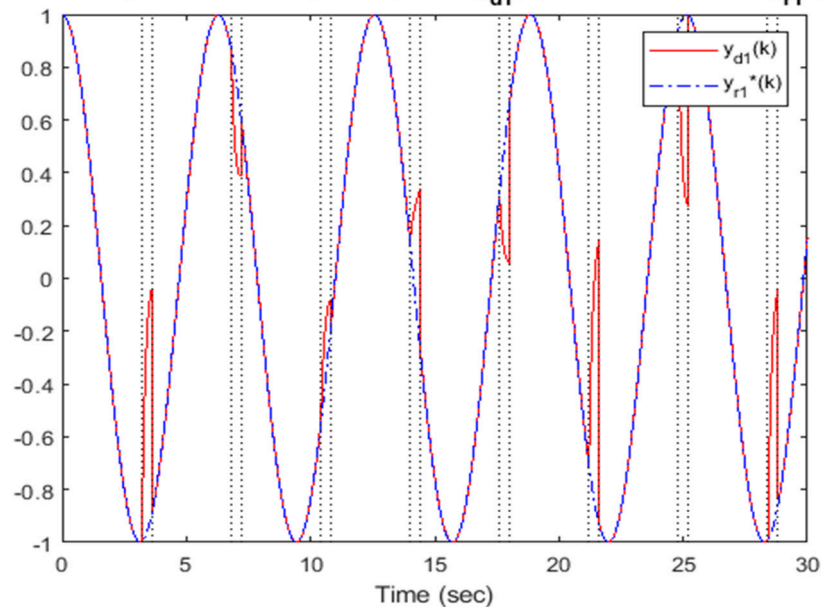
(b)

Figure 3. (a) The output response $y_{d1}(k)$ and the reference $y_{r1}^*(k)$, (b) The output response $y_{d2}(k)$ and the reference $y_{r2}^*(k)$.

From Figure 3a,b, we know that the MIMO discrete-time switched system (103) output responses $y_{d1}(k)$ and $y_{d2}(k)$ are bounded in the intervals $[-0.99, 0.99]$ and $[-0.44, 3.25]$. Thus, we can bound the output response in a certain range. The next consideration is the initial state $x_d(0) \neq 0$ in the system (103). Additionally, we use the same conditions (y_r^* , T and the simulation time) as in Figure 3 to get the simulation results in Figure 4a,b.

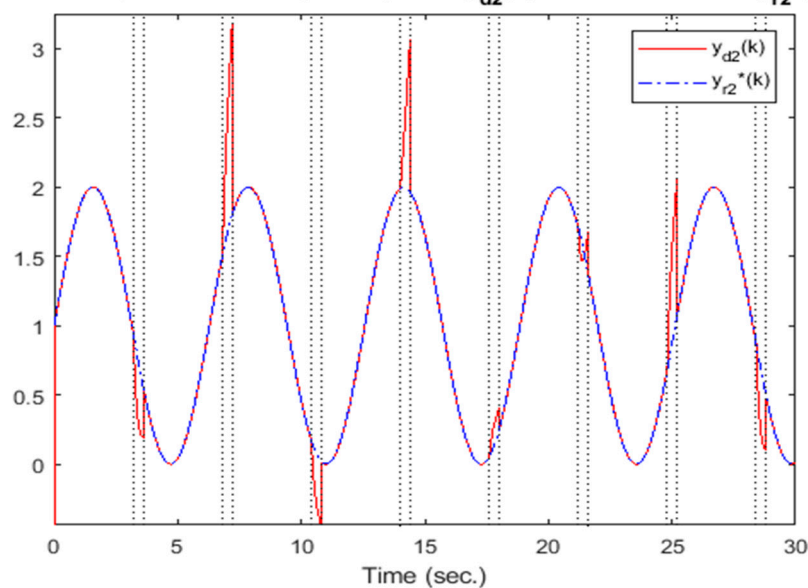
For system (103), the switching laws are the same whether $x_d(0) = 0$ or not, and we set $x_d = [1 \quad -0.7 \quad 0]$ to simulate as follows (Figure 4a,b):

The comparisons of output response $y_{d1}(k)$ and the reference $y_{r1}^*(k)$



(a)

The comparisons of output response $y_{d2}(k)$ and the reference $y_{r2}^*(k)$



(b)

Figure 4. (a) The output response $y_{d1}(k)$ and the reference $y_{r1}^*(k)$. (b) The output response $y_{d2}(k)$ and the reference $y_{r2}^*(k)$.

From Figure 4a,b, we know that the MIMO discrete-time switched system (103) output responses $y_{d1}(k)$ and $y_{d2}(k)$ are bounded in the intervals $[-0.99, 1]$ and $[-0.7, 3.25]$. Next, for different Q ($R = I_2$) selections, the robust performance and tracking performance are shown in Figures 5–8 and Table 1.

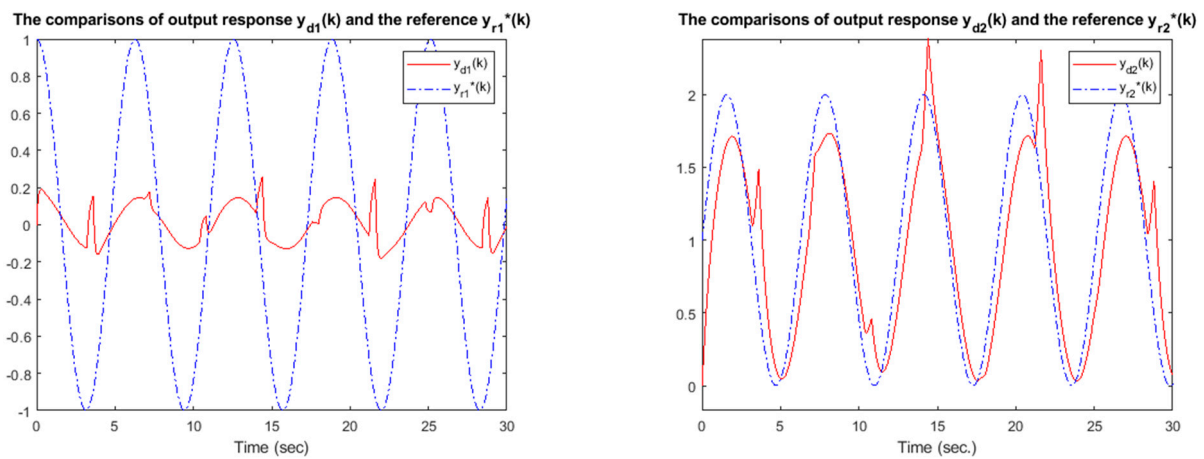


Figure 5. $Q = 10 \times I_2$: the robust performance and tracking performance.

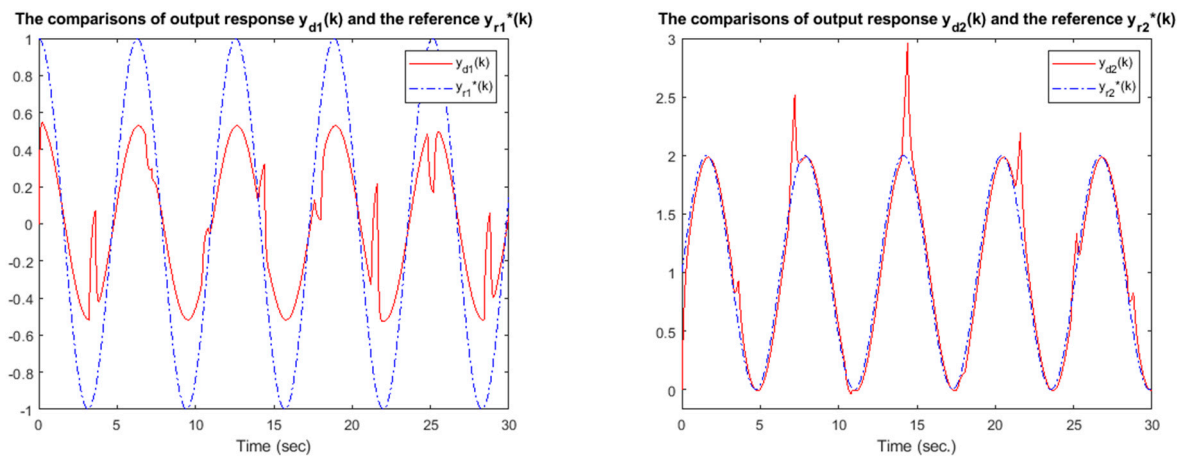


Figure 6. $Q = 10^2 \times I_2$: the robust performance and tracking performance.

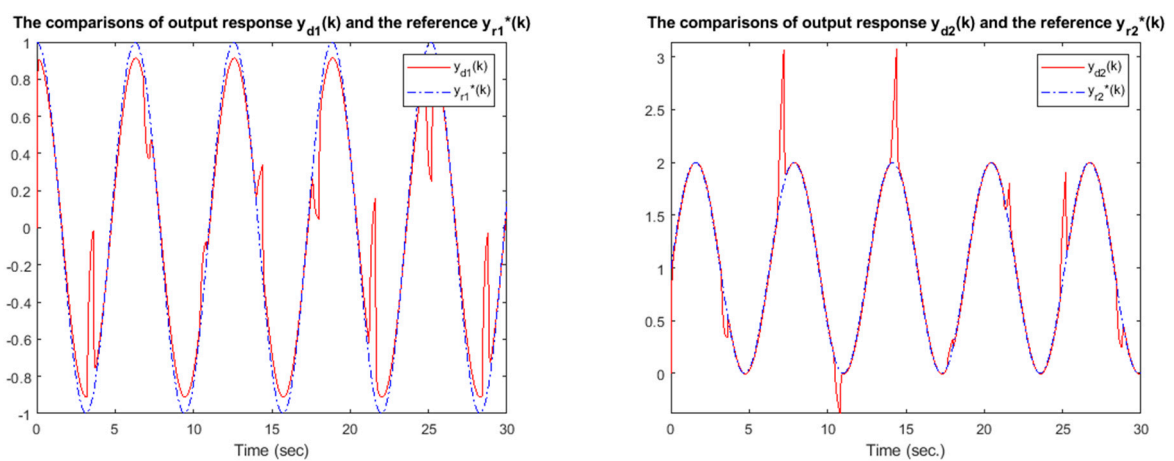


Figure 7. $Q = 10^3 \times I_2$: the robust performance and tracking performance.

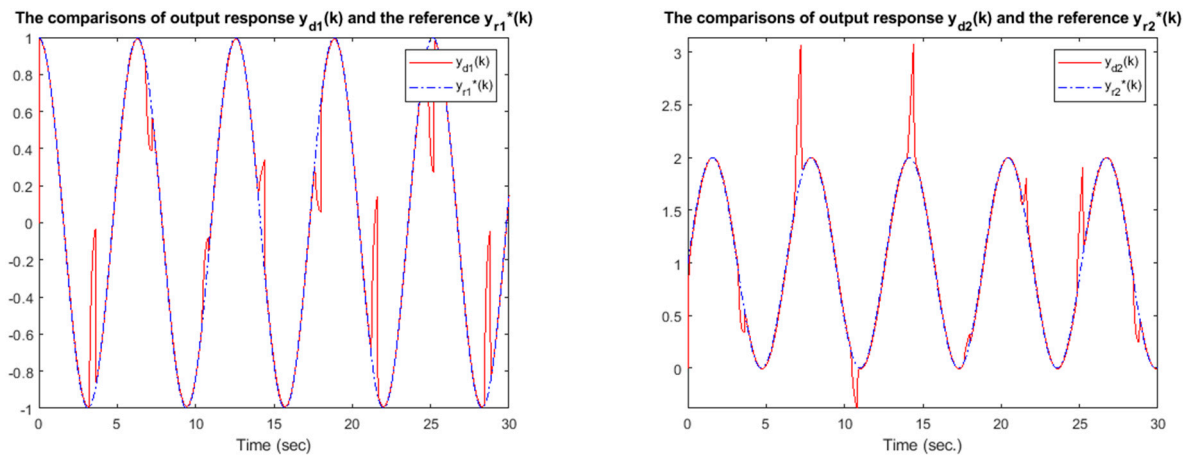


Figure 8. The robust performance and tracking performance.

Table 1. The robust performance and tracking performance comparison for different Q values.

Q	Bounded in the Intervals	Tracking Performance
$Q = 10 \times I_2$	$y_{d1}(k) : [-0.17, 0.26]$ $y_{d2}(k) : [0, 2.38]$	poor
$Q = 10^2 \times I_2$	$y_{d1}(k) : [-0.53, 0.53]$ $y_{d2}(k) : [-0.03, 2.97]$	poor
$Q = 10^3 \times I_2$	$y_{d1}(k) : [-0.9, 0.91]$ $y_{d2}(k) : [-0.38, 3.14]$	acceptable
$Q = 10^4 \times I_2$	$y_{d1}(k) : [-0.99, 0.99]$ $y_{d2}(k) : [-0.45, 3.26]$	good
$Q = 10^5 \times I_2$	$y_{d1}(k) : [-0.99, 0.99]$ $y_{d2}(k) : [-0.44, 3.25]$	good

6. Conclusions

This paper successfully derives switching laws by H_∞ linear matrix inequality for unstable discrete-time switched systems (61) and proves that state error (90) can be bounded. Because state error (90) is bounded, the system performance can also be bounded in a certain range. That tells us whether the controller will work or fail for an unstable discrete-time switched system (61), and we can know beforehand the approximate bound of system performance, which will be our expectation or not. However, we must note that P_s in the H_∞ linear matrix inequality might not have a solution, so it is necessary to choose appropriate parameters. In this paper, when the controller fails, we consider the controller to be zero, which denotes that all control signals are broken, and this is the worst situation. In the future, we will study when the controller fails and only several control factors are lost and use the method in this paper for further discussion.

Funding: This research was funded by National of Science and Technology Council of the Republic of China, Taiwan, for financially/partially supporting, grant number NSTC 111-2221-E-027-149.

Data Availability Statement: Not applicable.

Conflicts of Interest: The author declares no conflict of interest.

Appendix A

Consider (66) and set $P_s = r_0^{-1} \Lambda_s$, which will obtain

$$\begin{aligned} & \begin{bmatrix} A_s^T P_s A_s - \lambda_s^2 P_s & A_s^T P_s B_s & C_s^T \\ B_s^T P_s A_s & B_s^T P_s B_s - r_0 I & D_s^T \\ C_s & D_s & -r_0 I \end{bmatrix} < 0 \\ = & \begin{bmatrix} \sqrt{r_0}^{-1} & 0 & 0 \\ 0 & 1 & 0 \\ 0 & 0 & 1 \end{bmatrix} \begin{bmatrix} A_s^T \Lambda_s A_s - \lambda_0^2 \Lambda_s & \sqrt{r_0}^{-1} A_s^T \Lambda_s B_s & \sqrt{r_0} C_s^T \\ \sqrt{r_0}^{-1} B_s^T \Lambda_s A_s & r_0^{-1} B_s^T \Lambda_s B_s - r_0 I & D_s^T \\ \sqrt{r_0} C_s & D_s & -r_0 I \end{bmatrix} \begin{bmatrix} \sqrt{r_0}^{-1} & 0 & 0 \\ 0 & 1 & 0 \\ 0 & 0 & 1 \end{bmatrix} < 0. \end{aligned}$$

The above inequality denotes that

$$\begin{bmatrix} A_s^T \Lambda_s A_s - \lambda_0^2 \Lambda_s & \sqrt{r_0}^{-1} A_s^T \Lambda_s B_s & \sqrt{r_0} C_s^T \\ \sqrt{r_0}^{-1} B_s^T \Lambda_s A_s & r_0^{-1} B_s^T \Lambda_s B_s - r_0 I & D_s^T \\ \sqrt{r_0} C_s & D_s & -r_0 I \end{bmatrix} < 0.$$

Similarly, the above inequality can be decomposed as

$$\begin{bmatrix} 1 & 0 & 0 \\ 0 & \sqrt{r_0}^{-1} & 0 \\ 0 & 0 & \sqrt{r_0} \end{bmatrix} \begin{bmatrix} A_s^T \Lambda_s A_s - \lambda_0^2 \Lambda_s & A_s^T \Lambda_s B_s & C_s^T \\ B_s^T \Lambda_s A_s & B_s^T \Lambda_s B_s - r_0^2 I & D_s^T \\ C_s & D_s & I \end{bmatrix} \begin{bmatrix} 1 & 0 & 0 \\ 0 & \sqrt{r_0}^{-1} & 0 \\ 0 & 0 & \sqrt{r_0} \end{bmatrix} < 0,$$

and then

$$\begin{bmatrix} A_s^T \Lambda_s A_s - \lambda_0^2 \Lambda_s & A_s^T \Lambda_s B_s & C_s^T \\ B_s^T \Lambda_s A_s & B_s^T \Lambda_s B_s - r_0^2 I & D_s^T \\ C_s & D_s & -I \end{bmatrix} < 0.$$

It has the following decomposition:

$$\begin{bmatrix} A_s^T \Lambda_s A_s - \lambda_0^2 \Lambda_s & A_s^T \Lambda_s B_s & C_s^T \\ B_s^T \Lambda_s A_s & B_s^T \Lambda_s B_s - r_0^2 I & D_s^T \\ C_s & D_s & -I \end{bmatrix} = \begin{bmatrix} I & A_{12} A_{22}^{-1} \\ 0 & I \end{bmatrix} \begin{bmatrix} \hat{\Delta} & 0 \\ 0 & A_{22} \end{bmatrix} \begin{bmatrix} I & 0 \\ A_{22}^{-1} A_{21} & I \end{bmatrix} < 0,$$

where

$$A_{11} = \begin{bmatrix} A_s^T \Lambda_s A_s - \lambda_0^2 \Lambda_s & A_s^T \Lambda_s B_s \\ B_s^T \Lambda_s A_s & B_s^T \Lambda_s B_s - r_0^2 I \end{bmatrix}, A_{12} = \begin{bmatrix} C_s^T \\ D_s^T \end{bmatrix}, A_{21} = [C_s \quad D_s], A_{22} = -I,$$

and $\hat{\Delta} = A_{11} - A_{12} A_{22}^{-1} A_{21}$. The matrix $\hat{\Delta}$ is the Schur complement of A_{22} in A . Represent the above inequality as

$$\hat{\Delta} = \begin{bmatrix} A_s^T \Lambda_s A_s - \lambda_0^2 \Lambda_s & A_s^T \Lambda_s B_s \\ B_s^T \Lambda_s A_s & B_s^T \Lambda_s B_s - r_0^2 I \end{bmatrix} - \begin{bmatrix} C_s^T \\ D_s^T \end{bmatrix} (I)^{-1} [C_s \quad D_s] < 0,$$

which is equivalent to (67).

Appendix B

From (67), the following inequality is satisfied

$$\begin{aligned} & \begin{bmatrix} 1 & 0 \\ 0 & C_s^T \end{bmatrix} \begin{bmatrix} A_s^T \Lambda_s A_s - \lambda_s^2 \Lambda_s + C_s^T C_s & A_s^T \Lambda_s B_s + C_s^T D_s \\ B_s^T \Lambda_s A_s + D_s^T C_s & B_s^T \Lambda_s B_s - r_0^2 I + D_s^T D_s \end{bmatrix} \begin{bmatrix} 1 & 0 \\ 0 & C_s \end{bmatrix} \\ = & \begin{bmatrix} A_s^T \Lambda_s A_s - \lambda_s^2 \Lambda_s + C_s^T C_s & A_s^T \Lambda_s B_s + C_s^T D_s \\ C_s^T B_s^T \Lambda_s A_s + C_s^T D_s^T C_s & C_s^T B_s^T \Lambda_s B_s + C_s^T D_s^T D_s - r_0^2 C_s^T C_s + C_s^T D_s^T D_s \end{bmatrix} < 0, \end{aligned}$$

thus

$$\begin{aligned} & \begin{bmatrix} x_d^T(k) & x_r^* T(k) \end{bmatrix} \left(\begin{bmatrix} A_s^T \Lambda_s A_s - \Lambda_s & A_s^T \Lambda_s (B_s C_s - I) + \Lambda_s \\ (B_s C_s - I)^T \Lambda_s A_s + \Lambda_s & (B_s C_s - I)^T \Lambda_s (B_s C_s - I) - \Lambda_s \end{bmatrix} + \right. \\ & \left. \begin{bmatrix} (1 - \lambda_s^2) \Lambda_s + C_s^T C_s & A_s^T \Lambda_s - \Lambda_s + C_s^T D_s C_s \\ \Lambda_s A_s - \Lambda_s + C_s^T D_s^T C_s & C_s^T B_s^T \Lambda_s + \Lambda_s B_s C_s - r_0^2 C_s^T C_s + C_s^T D_s^T D_s \end{bmatrix} \right) \begin{bmatrix} x_d(k) \\ x_r^*(k) \end{bmatrix} < 0. \end{aligned}$$

Thus, (69) becomes

$$\begin{aligned}
 & V(x_d(k+1)) - V(x_d(k)) \\
 &= \begin{bmatrix} x_d^T(k) & x_r^{*T}(k) \end{bmatrix} \begin{bmatrix} A_s^T \Lambda_s A_s - \Lambda_s & A_s^T \Lambda_s (B_s C_s - I) + \Lambda_s \\ (B_s C_s - I)^T \Lambda_s A_s + \Lambda_s & (B_s C_s - I)^T \Lambda_s (B_s C_s - I) - \Lambda_s \end{bmatrix} \begin{bmatrix} x_d(k) \\ x_r^*(k) \end{bmatrix} \\
 &\leq - \begin{bmatrix} x_d^T(k) & x_r^{*T}(k) \end{bmatrix} \begin{bmatrix} (1 - \lambda_s^2) \Lambda_s + C_s^T C_s & A_s^T \Lambda_s - \Lambda_s + C_s^T D_s C_s \\ \Lambda_s A_s - \Lambda_s + C_s^T D_s^T C_s & C_s^T B_s^T \Lambda_s + \Lambda_s B_s C_s - r_0^2 C_s^T C_s + C_s^T D_s^T D_s C_s \end{bmatrix} \begin{bmatrix} x_d(k) \\ x_r^*(k) \end{bmatrix}
 \end{aligned}$$

where $D_s = 0$. The above matrix can be decomposed as

$$\begin{bmatrix} -C_s^T C_s & -A_s^T \Lambda_s \\ -\Lambda_s A_s & -(\Lambda_s B_s C_s + C_s^T B_s^T \Lambda_s) \end{bmatrix} = \begin{bmatrix} I & \varphi_{12} \varphi_{22}^{-1} \\ 0 & I \end{bmatrix} \begin{bmatrix} \hat{\Delta}_\varphi & 0 \\ 0 & \varphi_{22} \end{bmatrix} \begin{bmatrix} I & 0 \\ \varphi_{22}^{-1} \varphi_{21} & I \end{bmatrix},$$

where $\varphi_{11} = -C_s^T C_s$, $\varphi_{12} = -A_s^T \Lambda_s$, $\varphi_{21} = -\Lambda_s A_s$, $\varphi_{22} = -(\Lambda_s B_s C_s + C_s^T B_s^T \Lambda_s)$, and $\hat{\Delta}_\varphi = \varphi_{11} - \varphi_{12} \varphi_{22}^{-1} \varphi_{21}$. If $(\Lambda_s B_s C_s + C_s^T B_s^T \Lambda_s)^{-1} < C_s^T C_s$, then $\varphi_{22} < 0$ and $\hat{\Delta}_\varphi < 0$, which implies

$$\begin{bmatrix} -C_s^T C_s & -A_s^T \Lambda_s \\ -\Lambda_s A_s & -(\Lambda_s B_s C_s + C_s^T B_s^T \Lambda_s) \end{bmatrix} = \begin{bmatrix} I & \varphi_{12} \varphi_{22}^{-1} \\ 0 & I \end{bmatrix} \begin{bmatrix} \hat{\Delta}_\varphi & 0 \\ 0 & \varphi_{22} \end{bmatrix} \begin{bmatrix} I & 0 \\ \varphi_{22}^{-1} \varphi_{21} & I \end{bmatrix} < 0.$$

By the above inequality can be represented as

$$\begin{aligned}
 V(x_d(k+1)) - V(x_d(k)) &< \begin{bmatrix} x_d^T(k) & x_r^{*T}(k) \end{bmatrix} \begin{bmatrix} (\lambda_s^2 - 1) \Lambda_s & \Lambda_s \\ \Lambda_s & r_0^2 C_s^T C_s \end{bmatrix} \begin{bmatrix} x_d(k) \\ x_r^*(k) \end{bmatrix} \\
 &= \begin{bmatrix} x_d^T(k) & x_r^{*T}(k) \end{bmatrix} \begin{bmatrix} \lambda_s^2 \Lambda_s & 0 \\ 0 & \Lambda_s \end{bmatrix} \begin{bmatrix} x_d(k) \\ x_r^*(k) \end{bmatrix} - V(x_d(k)) + r_0^2 x_r^{*T}(k) C_s^T C_s x_r^*(k).
 \end{aligned}$$

Because

$$\begin{bmatrix} \lambda_s^2 \Lambda_s & 0 \\ 0 & \Lambda_s \end{bmatrix} \leq \begin{bmatrix} (\lambda_s^2 + 1) \Lambda_s & 0 \\ 0 & (\lambda_s^2 + 1) \Lambda_s \end{bmatrix},$$

It can be represented as

$$\begin{aligned}
 & V(x_d(k+1)) - V(x_d(k)) \\
 &\leq \begin{bmatrix} x_d^T(k) & x_r^{*T}(k) \end{bmatrix} \begin{bmatrix} (\lambda_s^2 + 1) \Lambda_s & 0 \\ 0 & (\lambda_s^2 + 1) \Lambda_s \end{bmatrix} \begin{bmatrix} x_d(k) \\ x_r^*(k) \end{bmatrix} - V(x_d(k)) + r_0^2 x_r^{*T}(k) C_s^T C_s x_r^*(k) \\
 &= \dots \\
 &\leq (\lambda_s^2 - 1) V(x_d(k)) + x_d^T(k) \Lambda_s x_d(k) + x_r^{*T}(k) \Lambda_s x_r^*(k) + r_0^2 x_r^{*T}(k) C_s^T C_s x_r^*(k) + \Psi,
 \end{aligned}$$

where the coupling terms $\Psi = \lambda_s^2 x_d^T(k) \Lambda_s x_r^*(k) + \lambda_s^2 x_r^{*T}(k) \Lambda_s x_d(k)$. The coupling terms Ψ can simplify as $\Psi = 2\lambda_s^2 x_r^{*T}(k) \Lambda_s x_r^*(k)$, because our target is $y_d(k) \rightarrow y_r^*(k)$, then $x_d(k) \rightarrow x_r^*(k)$.

Thus,

$$\begin{aligned}
 & V(x_d(k+1)) - V(x_d(k)) \\
 &\leq (\lambda_s^2 - 1) V(x_d(k)) + x_d^T(k) \Lambda_s x_d(k) + (2\lambda_s^2 + 1) x_r^{*T}(k) \Lambda_s x_r^*(k) + r_0^2 x_r^{*T}(k) C_s^T C_s x_r^*(k) \\
 &= (\lambda_s^2 - 1) V(x_d(k)) + x_d^T(k) C_s^T P_x C_s x_d(k) + (2\lambda_s^2 + 1) x_r^{*T}(k) C_s^T P_x C_s x_r^*(k) + r_0^2 x_r^{*T}(k) C_s^T C_s x_r^*(k) \\
 &= (\lambda_s^2 - 1) V(x_d(k)) + y_d^T(k) P y_d(k) + (2\lambda_s^2 + 1) y_r^{*T}(k) P y_r^*(k) + r_0^2 y_r^{*T}(k) y_r^*(k) \\
 &= (\lambda_s^2 - 1) V(x_d(k)) + \begin{bmatrix} y_d^T(k) & y_r^{*T}(k) \end{bmatrix} \begin{bmatrix} P & 0 \\ 0 & (2\lambda_s^2 + 1) P \end{bmatrix} \begin{bmatrix} y_d(k) \\ y_r^*(k) \end{bmatrix} + r_0^2 y_r^{*T}(k) y_r^*(k).
 \end{aligned}$$

The matrix

$$\begin{bmatrix} P & 0 \\ 0 & (2\lambda_s^2 + 1) P \end{bmatrix} \geq \begin{bmatrix} -cI & 0 \\ 0 & (2\lambda_s^2 + 1) \alpha I \end{bmatrix},$$

Finally, we can obtain (70) by the above result and its solution (71).

References

1. Xue, M.; Tang, Y.; Ren, W.; Qian, F. Stability of multi-dimensional switched systems with an application to open multi-agent systems. *Automatica* **2022**, *146*, 110644. [[CrossRef](#)]
2. Li, F.P.; Wang, R.H.; Fei, S.M. Stability and controller design of discrete-time switched systems based on transferring-dependent Lyapunov function approach. *Int. J. Control Autom. Syst.* **2022**, *20*, 1142–1153. [[CrossRef](#)]
3. Qi, S.; Zhao, J.; Tang, L. Adaptive output feedback control for constrained switched systems with input quantization. *Mathematics* **2023**, *11*, 788. [[CrossRef](#)]
4. Lin, X.; Huang, J.; Park, J. Finite-time non-smooth stabilization of cascade output-constrained switched systems. *Int. J. Robust Nonlinear Control* **2023**, *33*, 1407–2507. [[CrossRef](#)]
5. Han, Y.; Zhao, Y.; Wang, P. Finite-time rate anti-bump switching control for switched systems. *Appl. Math. Comput.* **2021**, *401*, 126086. [[CrossRef](#)]
6. Liberzon, D. *Switching in Systems and Control*, 1st ed.; Birkhäuser: Boston, MA, USA, 2003.
7. Sun, Z.; Ge, S.S. *Switched Linear Systems: Control and Design*, 1st ed.; Springer: London, UK, 2005.
8. Liu, X.; Zhong, S.; Ding, X. A Razumikhin approach to exponential admissibility of switched descriptor delayed systems. *Appl. Math. Model.* **2014**, *38*, 1647–1659. [[CrossRef](#)]
9. Lu, A.Y.; Yang, G.H. Stabilization of switched systems with all modes unstable via periodical switching laws. *Automatica* **2020**, *122*, 109150. [[CrossRef](#)]
10. Yu, Q.; Lv, H. Stability analysis for discrete-time switched systems with stable and unstable modes based on a weighted average dwell time approach. *Nonlinear Anal. Hybrid Syst.* **2020**, *38*, 100949. [[CrossRef](#)]
11. Sun, Z. Feedback stabilization of third-order switched linear control systems. *IEEE Control Syst. Lett.* **2020**, *4*, 857–861. [[CrossRef](#)]
12. Kundu, A.; Chatterjee, D. On stability of discrete-time switched systems. *Nonlinear Anal. Hybrid Syst.* **2017**, *23*, 191–210. [[CrossRef](#)]
13. Wang, R.H.; Jiao, T.C.; Zhang, T.; Fei, S.M. Improved stability results for discrete-time switched systems: A multiple piecewise convex Lyapunov function approach. *Appl. Math. Comput.* **2019**, *353*, 54–65. [[CrossRef](#)]
14. Zhao, X.; Shi, P.; Yin, Y.; Nguang, S.K. New results on stability of slowly switched systems: A multiple discontinuous Lyapunov function approach. *IEEE Trans. Automat. Control* **2016**, *62*, 3502–3509. [[CrossRef](#)]
15. Zhang, G.; Wang, L.; Li, J.; Zhang, W. Improved LVS guidance and path-following control for unmanned sailboat robot with the minimum triggered setting. *Ocean Eng.* **2023**, *272*, 113860. [[CrossRef](#)]
16. Bertolin, A.L.J.; Oliveira, R.C.L.F.; Valmorbidia, G.; Peres, P.L.D. An LMI approach for stability analysis and output-feedback stabilization of discrete-time Lur'e systems using Zames-Falb multipliers. *IEEE Contr. Syst. Lett.* **2022**, *6*, 710–715. [[CrossRef](#)]
17. Li, X.; de Souza, C.E. Delay-dependent robust stability and stabilization of uncertain linear delay systems: A linear matrix inequality approach. *IEEE Trans. Autom. Control* **1997**, *42*, 1144–1148. [[CrossRef](#)]
18. Zhang, L.; Shi, P. Stability, L₂–Gain and asynchronous H_∞ control of discrete-time switched systems with average dwell time. *IEEE Trans. Autom. Control* **2009**, *54*, 2192–2199. [[CrossRef](#)]
19. Zhao, X.D.; Zhang, L.X.; Shi, P.; Liu, M. Stability and stabilization of switched linear systems with mode-dependent average dwell time. *IEEE Trans. Automat. Control* **2012**, *46*, 1809–1815. [[CrossRef](#)]
20. Li, Y.; Zhang, H. Dwell time stability and stabilization of interval discrete-time switched positive linear systems. *Nonlinear Anal. Hybrid Syst.* **2019**, *33*, 116–129. [[CrossRef](#)]
21. Du, S.L.; Karimi, H.R.; Qiao, J.F.; Wu, D.; Feng, C. Stability analysis for a class of discrete-time switched systems with partial unstable subsystems. *IEEE Trans. Circuit. Syst. II Express Briefs* **2019**, *66*, 2017–2021. [[CrossRef](#)]
22. Zhai, G.; Hu, B.; Yasuda, K.; Michel, A.N. Qualitative analysis of discrete-time switched systems. In Proceedings of the American Control Conference, Anchorage, AK, USA, 8–10 May 2002.
23. Hespanha, J.P.; Morse, A.S. Stability of switched systems with average dwell-time. In Proceedings of the 38th IEEE Conference on Decision and Control, Phoenix, AZ, USA, 7–10 December 1999.
24. Zhai, G.; Lin, H.; Xu, X.; Imae, J.; Kobayashi, T. Analysis of switched normal discrete-time systems. In Proceedings of the American Control Conference, Portland, OR, USA, 8–10 June 2005.
25. Wicks, M.A.; Peleties, P.; DeCarlo, R.A. Construction of piecewise Lyapunov functions for stabilizing switched systems. In Proceedings of the 33rd IEEE Conference on Decision and Control, Lake Buena Vista, FL, USA, 14–16 December 1994.
26. Lee, L.; Chen, J.L. Strictly positive real lemma and absolute stability for discrete-time descriptor systems. *IEEE Trans. Circuits Syst. I Fundam. Theory Appl.* **2003**, *50*, 788–794. [[CrossRef](#)]
27. Peters, A.A.; Vargas, F.J.; Chen, J. An algebraic formula for performance bounds of a weighted H_∞ optimal control problem. *IEEE Trans. Automat. Control* **2021**, *66*, 781–786. [[CrossRef](#)]
28. Brogliato, B.; Lozano, R.; Maschke, B.; Egeland, O. *Dissipative Systems Analysis and Control*, 3rd ed.; Springer: Cham, Switzerland, 2020.
29. Iwasaki, T.; Skelton, R.E.; Grigoriadis, K.M. *A Unified Algebraic Approach to Linear Control Design*; Taylor & Francis: London, UK, 1998.
30. Guo, S.M.; Shieh, L.S.; Chen, G.; Lin, C.F. Effective chaotic orbit tracker: A prediction-based digital redesign approach. *IEEE Trans. Circuits Syst. I Fundam. Theory Appl.* **2000**, *47*, 1557–1570.
31. Tsai, J.S.H.; Chen, F.M.; Guo, S.M.; Chen, C.W.; Shieh, L.S. A novel tracker for a class of sampled-data nonlinear systems. *J. Vib. Control* **2011**, *17*, 81–101. [[CrossRef](#)]

32. Shieh, L.S.; Wang, W.M.; Zheng, J.B. Robust control of sampled-data uncertain systems using digitally redesigned observer-based controller. *Int. J. Control* **1997**, *66*, 43–64. [[CrossRef](#)]
33. Guo, S.M.; Shieh, L.S.; Lin, C.F.; Chandra, J. State-space self-tuning control for nonlinear stochastic and chaotic hybrid systems. *Int. J. Bifurcation Chaos* **2001**, *11*, 1079–1113. [[CrossRef](#)]
34. Zhai, G.; Chen, X.; Takai, S.; Yasuda, K. Stability and H_∞ disturbance attenuation analysis for LTI control systems with controller failures. *Asian J. Control* **2004**, *6*, 104–111.
35. Xiang, W.; Tran, H.D.; Johnson, T.T. Nonconservative lifted convex conditions for stability of discrete-time switched systems under minimum dwell-time constraint. *IEEE Trans. Autom. Control* **2019**, *64*, 3407–3414. [[CrossRef](#)]

Disclaimer/Publisher’s Note: The statements, opinions and data contained in all publications are solely those of the individual author(s) and contributor(s) and not of MDPI and/or the editor(s). MDPI and/or the editor(s) disclaim responsibility for any injury to people or property resulting from any ideas, methods, instructions or products referred to in the content.